Metal and Multimetal Complexes with Polyaromatic Hydrocarbons: Formation and Photodissociation of Fe_x−(Coronene)$_y$ Cations

J. W. Buchanan, J. E. Reddic, G. A. Grieves, and M. A. Duncan*

Department of Chemistry, University of Georgia, Athens, Georgia 30602

Received: March 17, 1998; In Final Form: June 3, 1998

Gas-phase cluster complexes containing coronene and iron are produced in a molecular beam and studied with time-of-flight mass spectrometry. Cation complexes are produced in a pulsed nozzle laser vaporization cluster source using a metal rod coated with a sublimed film of coronene. Cluster masses of the form $[Fe_x-cor_y]^+$ are observed for $x = 1-3$ and $y = 1,2$. Additional masses are observed for the complexes $[Fe-cor_y]^+$ for $y = 1-7$. Mass-selected laser photodissociation experiments probe the structure and bonding in these new cluster species. Evidence is presented for stable sandwich structures and for the existence of multi-iron species as separated atoms on the coronene surface.

Introduction

The multicentered bonding exhibited by organometallic π complexes has stimulated interest for many years.[1−3] Recently, new techniques have made it possible to synthesize fascinating new complexes in the gas phase and to investigate their spectroscopy and photochemistry. Numerous studies have investigated metal benzene complexes or those with other small aromatic systems.[2−9] More recently, molecular beam experiments have produced remarkable multi-decker metal complexes with benzene.[9] Mass spectrometry experiments have also produced metal complexes with larger aromatic systems including polyaromatic hydrocarbons (PAH's)[10] and fullerenes.[11−16] With laser or oven sources designed for higher metal densities, multiple metal atom films have been produced on the surface of C_{60}[14−16] and metal−C_{60}-metal−C_{60} networks have been produced.[16] These species exhibit unusual bonding and they are expected to have interesting optical properties, although these measurements have not yet been investigated. In the present report, we describe the production of complexes combining multiple metal atoms (iron) with the PAH system coronene ($C_{24}H_{12}$; mol. wt. 300; see Figure 4 below). Because of the extended aromatic system in coronene, multiple binding sites are present presenting varied possibilities for organometallic bonding. It is also conceivable that binding could occur on both sides of the coronene ring system. Production of multi-metal/multi-coronene complexes makes it possible to explore these new bonding possibilities for the first time. We demonstrate a general method to produce metal/PAH clusters, and we investigate their photodissociation dynamics.

Polyaromatic hydrocarbons are present in a variety of natural environments such as sooty flames. Their stability is such that they can survive at high temperatures. The optical properties of these systems have been investigated in solution, in high-temperature gases and in cryogenic matrices.[17−26] Neutral and/or cation PAH species have been proposed as carriers for the unidentified infrared lines (UIR's) or the optical diffuse interstellar bands (DIB's).[19,20] However, recent studies have shown that the measured spectra of isolated PAH molecules or their ions do not match precisely with the astrophysical spectra, especially with regard to oscillator strengths.[19−26] Complexes with PAH species, including those containing metals, have been proposed as alternative carriers for the unidentified spectra.[18] However, a general source of gas-phase PAH molecules and/or complexes in neutral or ionized form at the required low temperatures of the interstellar medium ($\leq$50 K) has not been available previously to test these proposals.

Coronene complexes with single metal atoms have been studied previously by Dunbar and co-workers.[10] Metal ions were produced by laser vaporization without a collision gas and interacted with a low pressure of sublimed coronene vapor in a Fourier transform mass spectrometer. Radiative association kinetics were measured for a variety of transition metal and main group metal cations. Addition of one or two coronene molecules to a single metal ion was observed. In the present study, metal−coronene complexes are produced by laser vaporization of a composite sample in a pulsed nozzle cluster source. These conditions yield more extensive clustering of both metal and coronene, and make it possible for the first time to produce multiple metal atoms and/or metal clusters bound to a single coronene moiety, as well as clusters containing both multiple metals and multiple coronene molecules. Species produced from this source are supersonically cooled, and the prospect exists for spectroscopic studies. In the present report, mass-selected photodissociation probes the structure and bonding in these novel organometallics.

Experimental Section

Iron−coronene complexes are produced in a laser vaporization cluster source with specially prepared samples. A pure iron rod is coated with a sublimed film of coronene on the surface. Films are deposited in a small vacuum chamber dedicated for sample preparation. A sublimation oven is constructed from a $^1/_4$ in. diameter ceramic tube wrapped with a Nichrome wire heater and controlled with a variac. Coronene powder (Aldrich) is heated until visible sublimation occurs on the vacuum chamber windows. The sample rod is mounted on a rotating stage about 2 in. from the oven. The resulting film thickness is approximately 0.1 mm.

---

* To whom correspondence should be addressed. E-mail: maduncan@uga.cc.uga.edu.

S1089-5639(98)01513-8 CCC: $15.00

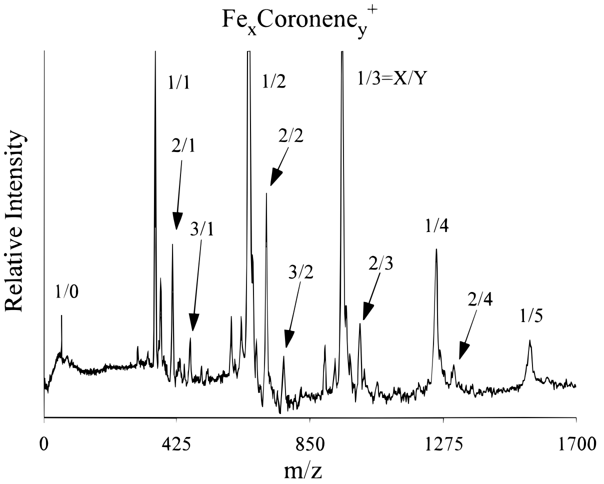

Figure 1. Mass distribution of iron−coronene cation complexes produced by laser vaporization of an iron rod coated with a film of coronene. The peaks labeled X, Y indicate the Fe$_x$−coronene$_y$ stoichiometries for the cation complexes.

The film-coated metal rod is transferred to a molecular beam machine and mounted in a rotating rod/laser vaporization cluster source. This source is of standard design but uses a modified Newport nozzle.[15] Vaporization is accomplished with the third harmonic of a Nd:YAG laser at 355 nm. We use laser powers lower than those typically employed for pure metal vaporization (about 10 mJ/pulse). The conditions are similar to those recently described for metal−C_{60} complex formation where signals are sensitive to both film thickness and the vaporization laser power.[15] Under optimized conditions the vaporization laser desorbs coronene and penetrates to ablate the underlying metal, thus producing both species in the gas phase. Complexes grow by recombination in the gas channel, which extends beyond the vaporization point. This growth channel is 1−2 cm in length and has a larger diameter (4 mm) than typically used to produce pure metal clusters. The cation clusters produced directly in the source pass through a skimmer and are extracted from the molecular beam into the mass spectrometer with pulsed acceleration voltages. The beam apparatus for these experiments was described previously.[5]

Results and Discussion

Figure 1 shows the mass spectrum measured when the coronene-coated iron rod is vaporized and the resulting cation clusters are sampled into the mass spectrometer. Under these conditions the naked coronene cation is formed with low relative abundance, and there is no evidence for bare iron clusters. With no coronene present, this same nozzle configuration is actually inefficient in producing bare iron clusters but instead produces large signals of the Fe^+ atomic ion. Bare iron cluster cations can be produced when there is no coronene present and the nozzle is configured with a longer and narrower channel beyond the vaporization point. When the coronene film is added, the most prominent masses are those corresponding to $[Fe-(cor)_y]^+$, where $y = 1-5$. For example, the most intense peak in the mass spectrum (independent of instrument focusing) is $[Fe-(cor)_2]^+$, which is off-scale in Figure 1. This immediately suggests the possibility of a sandwich structure. Additional masses are seen for multiple iron adducts with each coronene increment, i.e., $[Fe_x-(cor)_y]^+$. For one or two coronenes, there are clear peaks for up to three iron atoms, i.e., 3/1 and 3/2, respectively. For larger coronene multiples, there are no more than two iron atoms.

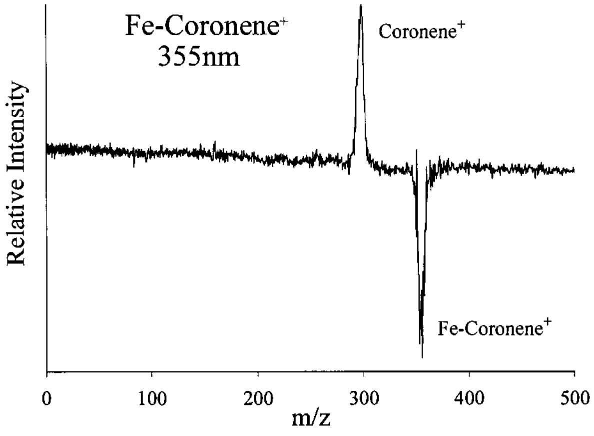

Figure 2. Photodissociation of the $[Fe-cor]^+$ complex at 355 nm. The coronene cation is the only fragment observed because coronene has a lower ionization potential than iron atom.

It is clear from these masses alone that multiple metal atoms have been attached to coronene molecules. From the dependence on source conditions, it is clear that iron−coronene mixed clusters, even those containing multiple iron atoms, form more readily than pure iron clusters. There is no evidence for destruction of coronene in the laser-generated plasma, consistent with our previous observation for metal−C_{60} complexes produced this same way.[15] There is also no evidence for reactive destruction of coronene by iron, which could conceivably produce smaller metal−hydrocarbon or metal−carbide masses. Under lower laser power conditions with thicker coronene films, PAH_y^+ cations without metal are easily observed. Neutral metal−PAH species are also produced, and these species can be detected with excimer laser photoionization (ArF; 193 nm; data not shown). This method therefore is general to produce neutral or cation PAH species in the cold molecular beam environment.

Photodissociation measurements on these clusters may provide information about their structures and bonding properties. For these measurements, we investigate the relative cross section for photodissociation, the wavelength dependence, if any, and the fragmentation channels. The most striking observation for all of the Fe_x-cor_y clusters formed is their resistance to photodissociation at all wavelengths studied (610, 532, and 355 nm). We have produced pure iron cluster cations (Fe_x^+; $x = 2-4$), and these species fragment with extremely high efficiency at all three of these wavelengths. Absolute cross sections are not readily obtained in our beam configuration, but we conclude that the *relative* cross sections for photodissociation of the Fe_x-cor_y clusters is at least an order of magnitude lower than those for small iron cluster cations. In each experiment on the Fe/coronene complexes, we necessarily use high-power laser excitation, and we therefore conclude that these photodissociation processes are multiphoton in nature. Therefore, the exact energy deposition is uncertain, but this in no way affects the interpretation of the fragmentation channels discussed below. In each cluster studied, fragmentation processes eliminate units of either 56 or 300 amu or combinations of these. Losses of mass 56 are attributed to iron atoms rather than two C_2H_4 groups because there is no obvious reason C_2H_4 should be eliminated in pairs. Additionally, there are only 12 hydrogen atoms in the parent complex, and multiple elimination of C_2H_4, as required to explain the loss of two or more units of 56 amu, is not possible.

We have studied photodissociation for the species $[Fe-cor_y]^+$ for $y = 1-4$. Figure 2 shows the photodissociation of [Fe−

TABLE 1: Energetics of Ionization and Fragmentation for Fe$_x$−Coronene Fragments

	ionization potential (eV)^{27}	dissociation energy (M$_x$−M)$^+$ (eV)^{28}
Fe	7.87	
Fe$_2$	6.30	2.72
Fe$_3$	6.4	1.64
coronene	7.29	

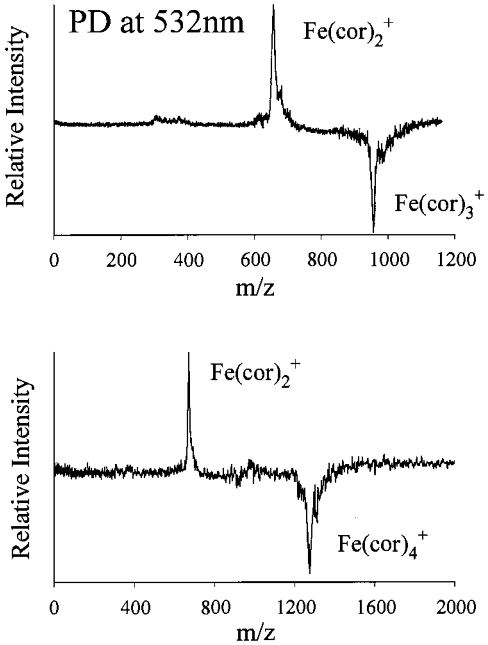

Figure 3. Photodissociation mass spectra of [Fe−cor$_3$]$^+$ and [Fe−cor$_4$]$^+$. The only fragment observed with significant intensity is [Fe−cor$_2$]$^+$, which is suggested to represent a sandwich complex.

cor]$^+$ at 355 nm. In these fragmentation spectra, the negative peak indicates destruction of the mass-selected parent ion while positive peaks indicate the charged photofragments. As indicated, this complex dissociates to produce the coronene cation (plus undetected neutral Fe). This same behavior is seen at both the 532 and 355 nm wavelengths. This fragmentation process is expected because coronene has a lower ionization potential (IP) than the iron atom (see Table 1). The charge in the complex is therefore expected to be delocalized primarily on the coronene, and dissociation yields the neutral metal atom and molecular ion along this lower energy path. Thus, even though the fragmentation process is multiphoton, the expected lowest energy channel is observed. This simple cleavage process demonstrates that the iron and coronene units retain their essential identity and that no extensive rearrangements, such as insertion of iron into the ring system, have taken place. In data not shown, [Fe−cor$_2$]$^+$ also dissociates to produce primarily the coronene cation. In this case the undetected neutral(s) could be either Fe−coronene or Fe + coronene. More interesting fragmentation processes are observed for the clusters [Fe−cor$_3$]$^+$ and [Fe−cor$_4$]$^+$. As shown in Figure 3, both of these species produce exclusively the [Fe−cor$_2$]$^+$ complex. The prominent production of this species in the distribution of ions grown by the source and its production from the fragmentation of larger clusters provide strong evidence for the special stability of [Fe−cor$_2$]$^+$. The logical assumption is that it represents a sandwich complex. A sandwich complex is naturally associated with π bonding, but there is nothing in our data to rule out the possibility of bridged bonding with the metal atom located over double bonds.

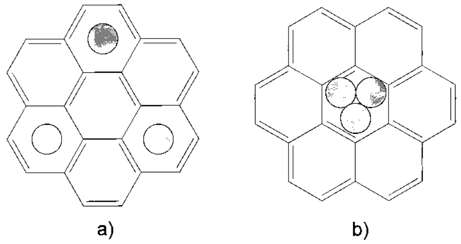

Figure 4. Two structural motifs considered for multi-iron coronene complexes: (a) dispersed metal atoms and (b) island formation.

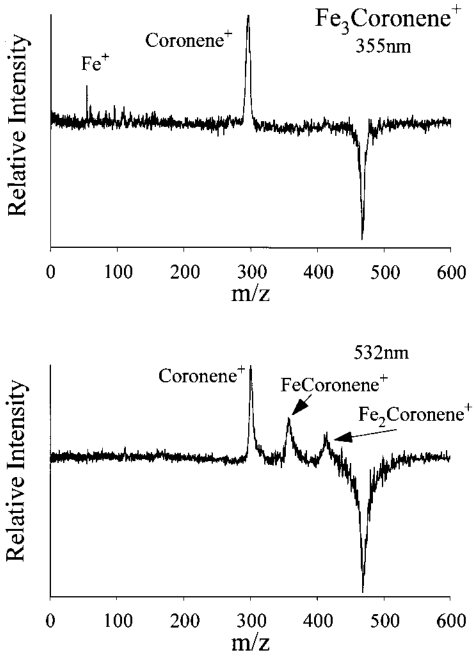

Figure 5. Photodissociation mass spectra for [Fe$_3$−coronene]$^+$ at 355 and 532 nm.

A fascinating aspect of these studies is the production of masses corresponding to multiple iron atoms bound to a single coronene molecule, as well as multi-iron−multi-coronene masses. These kinds of complexes have not been produced previously, and immediate questions are raised about their structure and bonding, which of course cannot be answered satisfactorily by mass spectrometry. Two general schemes are possible for multimetal attachment to the flat surface of the coronene molecule, which are demonstrated in Figure 4 for the Fe$_3$-coronene species. The metals may disperse over the coronene surface and bind to various ring sites via individual π or bridging interactions. The figure shows the π sites occupied rather than bridged sites only because of drawing convenience. It is also conceivable that such interactions could take place on both sides of the coronene surface. The other possibility shown is that multiple atoms may cluster into an "island" on the coronene surface. Both of these motifs are familiar for metals on bulk surfaces, but these considerations are new for metals on "molecular surfaces." To attempt to investigate these structural possibilities we use mass-selected photodissociation of these clusters.

Figure 5 shows the photodissociation mass spectra of [Fe$_3$−coronene]$^+$ at 355 and 532 nm. [Fe$_2$−coronene]$^+$ has similar fragmentation products at these two wavelengths. First of all, it is important to mention that the photodissociation cross section is extremely small for both of these clusters at both 355 and 532 nm. In the same way seen for the other clusters above, fragmentation occurs only at high laser powers and is believed to be multiphoton in nature. At 610 nm, the laser power available is less and no fragmentation is detected. At 355 nm, both the $[Fe_2{-}coronene]^+$ and $[Fe_3{-}coronene]^+$ complexes produce the coronene cation as the main charged fragment, with a small amount of Fe^+ also observed. These data clearly indicate that the metal atoms and/or clusters bound to the coronene surface have been completely removed. Four channels are possible for these elimination processes involving the ejection of atomic or molecular iron fragments:

$$[Fe_x{-}coronene]^+ \rightarrow coronene^+ + Fe_x, Fe_{x-1}, \text{etc.} \quad \text{(neutral molecular metal)} \quad (1)$$

$$[Fe_x{-}coronene]^+ \rightarrow coronene + Fe_x{}^+, Fe_{x-1}{}^+, \text{etc.} \quad \text{(charged molecular metal)} \quad (2)$$

$$[Fe_x{-}coronene]^+ \rightarrow coronene^+ + xFe \quad \text{(neutral atomic metal)} \quad (3)$$

$$[Fe_x{-}coronene]^+ \rightarrow coronene + Fe^+ + (x-1)Fe \quad \text{(charged atomic metal)} \quad (4)$$

Of these, channel 2 can be ruled out because $Fe_2{}^+$ or $Fe_3{}^+$ are not observed under any conditions. Further insight can be gained because the ionization and fragmentation energetics of small iron clusters are known from previous studies (see Table 1).[27,28] Significantly, the iron atom has a *higher* IP (7.87 eV) than the coronene molecule (7.29 eV), while both Fe_2 and Fe_3 have *lower* IP's than coronene. Therefore, if diatomic or triatomic iron molecules are ejected from the coronene complexes, these molecular iron species should be charged and the corresponding coronene should be neutral. Channel 1 can therefore be eliminated. The conclusion is that channel 3 or channel 4, which involve the ejection of *atomic* iron fragments, are the only fragmentation processes observed for both $[Fe_2{-}coronene]^+$ and $[Fe_3{-}coronene]^+$. The Fe^+ signal detected is quite weak, and it is not seen at 532 nm. The small Fe^+ signal at 355 nm is consistent with the photoionization of neutral iron atoms by continued absorption in the high-power laser field, rather than by the direct ejection of Fe^+. The direct ejection of Fe^+ is also not expected because the IP of Fe is greater than that of coronene. The coronene cation is prominent under all conditions. Therefore, we conclude that channel 4 can be ruled out also and that channel 3 represents the primary fragmentation process for these complexes.

This fragmentation channel is even clearer in the data at 532 nm, where the intermediate $[Fe_x{-}coronene]^+$ fragments are observed in addition to the coronene cation. Elimination of neutral iron atoms, either sequentially or in parallel, is therefore again indicated with no evidence for $Fe_2{}^+$ or $Fe_3{}^+$ fragments. The 532 nm photon deposits less energy than the 355 nm photon, and so the fragmentation process is apparently captured at an intermediate stage. The broadening in these fragment peaks is not caused by instrument resolution. Instead, we attribute it to a metastable component in the fragmentation processes, which indicates that dissociation takes place on about the same time scale as acceleration out of the reflectron region (1−2 μs). Therefore, it is again concluded that fragmentation of $[Fe_2{-}coronene]^+$ and $[Fe_3{-}coronene]^+$ occurs by elimination of neutral iron atoms.

The photodissociation dynamics and cross sections for these clusters provide strong circumstantial evidence about their structure and bonding. As indicated in Figure 4, it is conceivable that the adsorbed iron in $[Fe_2{-}coronene]^+$ and $[Fe_3{-}coronene]^+$ exists as clusters or as separated atoms. If these complexes had adsorbed iron clusters, we might expect that the efficiency of photodissociation would be similar to that of isolated iron clusters, but it is not. As described, isolated iron clusters dissociate efficiently at 610, 532, and 355 nm, while the complexes here have cross sections at least an order of magnitude weaker at these wavelengths. If sufficient energy is present to break all bonds, it is a lower energy process to eliminate *molecular* iron species than it is to eliminate atoms.[29] As shown in Figure 5, in both the 355 and 532 nm data enough energy is deposited to completely remove all the metal from all (355 nm) or at least some of (532 nm) the clusters, but no molecular fragments are observed. If the iron atoms in these dissociation processes are bound to each other, or even perhaps just physically close to each other, then at least some of the lower energy molecular fragments should be formed, but they are not. Efficient elimination of molecular metal fragments has been observed in other multimetal coronene complexes (chromium, nickel) that we have studied.[30] Iron is thus different from these other transition metals in this regard. Unusual resonance effects can be ruled out here because the photochemistry is essentially the same (in the sense of no molecular metal fragments) at both wavelengths studied. Additionally, the tailing in the mass spectra peaks indicate that dissociation is occurring on the microsecond time scale where the energetically lower pathways for decomposition are favored (as opposed to fast dissociation on repulsive excited states). The conclusion from these observations is that the iron atoms are not in close proximity, and therefore elimination of molecular metal fragments is not possible dynamically. In other words, the metal in these two- and three-iron complexes is dispersed to form individual atomic interactions with the coronene surface. These systems therefore represent an unusual new form of organometallic bonding. Metal attachment at two separated sites on the surface of polyaromatic hydrocarbons has been observed previously in the condensed phase chemistry of iron cyclopentadiene in so-called bis-arene π complexes.[31,32] However, gas-phase species with multiple isolated metal atoms have not been observed previously.

Although we can conclude that the multi-iron species have separately adsorbed atoms, our data does not provide information about the specific location of these atoms, including whether the metals are located in π sites, whether they are on the same side of the molecule, or whether there is a distribution of structural isomers. However, one particularly attractive structure for the $[Fe_3{-}coronene]^+$ complex places the metals in equivalent positions on alternating rings, as shown in Figure 4. This structure maximizes the separation between the metal atoms and minimizes the disruption of the π bonding network in the ring system. Interestingly, in mass spectra measured so far, we have only detected strong peaks for complexes with up to three metal atoms, regardless of the number of coronene rings present. For example, the double-coronene mass region shows that up to three irons are added here as well. It is therefore interesting to speculate about the possibility of di- and tri-iron sandwich structures. Simple molecular modeling shows that three iron atoms are large enough to cover a sizable fraction of the coronene surface. However, additional experiments will be required to determine whether the cutoff at three atoms indicates special bonding stability (i.e., total coverage) or simply an effect of limited metal density.

Conclusion

We have shown that neutral and ionic complexes of iron and coronene can be produced in a supersonic molecular beam environment by laser vaporization of a film-coated metal rod. Photodissociation of $[\mathrm{Fe{-}cor}_y]^+$ complexes produce $[\mathrm{Fe{-}cor}_2]^+$ as a prominent fragment, and this species is also produced preferentially from the source, suggesting that it is a stable sandwich complex. Experiments on $[\mathrm{Fe}_x\mathrm{{-}cor}]^+$ complexes ($x = 2, 3$) demonstrate that iron binds to intact coronene molecules and that these systems eliminate neutral metal atoms rather than molecular metal fragments as they decompose. This indicates that the metal on the surface of coronene is present as separated atoms interacting individually with the coronene π system. These complexes represent a novel form of organometallic bonding, which has not been investigated previously with experiments or theory. These complexes are also appealing models for theory corresponding to "metal monolayer films" adsorbed on "molecular surfaces." Analogies may also be possible with metal-intercalated graphite. Future studies will investigate the optimization of the source to produce larger metal-coronene aggregates and the optical spectroscopy of these new systems. We have performed this same kind of experiment with silver, chromium, nickel, calcium, and niobium in complexes with coronene. We have also investigated metal−phenanthrene, pyrene, and perylene complexes. Similar mass spectra are obtained with these other metals and other PAH molecules. However, the fragmentation patterns observed here for iron are unique among the systems studied so far, indicating strong binding of separated atoms in the multimetal complexes. The methodology described here is general for the production of many kinds of metal−PAH complexes in the supersonic molecular beam environment. This source is also convenient for the production of PAH neutral and/or cation clusters without metal. Future studies will investigate the photodissociation and photoionization dynamics of these new systems.

Acknowledgment. This research is supported by the Air Force Office of Scientific Research through Grant F49620-94-0063 and the National Science Foundation through Grant CHE-9529043. We appreciate helpful discussions with Professors Charles Kutal and R. B. King.

References and Notes

(1) Mulliken, R. S.; Person, W. B. *Molecular Complexes*; Wiley-Interscience: New York, 1969.

(2) (a) Ma, J. C.; Dougherty, D. A. *Chem. Rev.* **1997**, *97*, 1303. (b) Dougherty, D. A. *Science* **1996**, *271*, 163.

(3) Caldwell, J. W.; Kollman, P. A. *J. Am. Chem. Soc.* **1995**, *117*, 4177.

(4) (a) Jacobson, D. B.; Freiser, B. S. *J. Am. Chem. Soc.* **1984**, *106*, 3900. (b) Jacobson, D. B.; Freiser, B. S. *J. Am. Chem. Soc.* **1984**, *106*, 4623. (c) Rufus, D.; Ranatunga, A.; Freiser, B. S. *Chem. Phys. Lett.* **1995**, *233*, 319. (d) Afzaal, S.; Freiser, B. S. *Chem. Phys. Lett.* **1994**, *218*, 254.

(5) (a) Willey, K. F.; Cheng, P. Y.; Bishop, M. B.; Duncan, M. A. *J. Am. Chem. Soc.* **1991**, *113*, 4721. (b) Willey, K. F.; Yeh, C. S.; Robbins, D. L.; Duncan, M. A. *J. Phys. Chem.* **1992**, *96*, 9106.

(6) (a) Chen, Y. M.; Armentrout, P. B. *Chem. Phys. Lett.* **1993**, *210*, 123. (b) Meyer, F.; Khan, F. A.; Armentrout, P. B. *J. Am. Chem. Soc.* **1995**, *117*, 9740.

(7) (a) Sodupe, M.; Bauschlicher, C. W. *J. Phys. Chem.* **1991**, *95*, 8640. (b) Sodupe, M.; Bauschlicher, C. W.; Langhoff, S. R.; Partridge, H. *J. Phys. Chem.* **1992**, *96*, 2118. (c) Bauschlicher, C. W.; Partridge, H.; Langhoff, S. R. *J. Phys. Chem.* **1992**, *96*, 3273. (d) Sodupe, M.; Bauschlicher. *Chem. Phys.* **1994**, *185*, 163.

(8) (a) Dunbar, R. C.; Klippenstein, S. J.; Hrusak, J.; Stöckigt, D.; Schwartz, H. *J. Am. Chem. Soc.* **1996**, *118*, 5277. (b) Ho, Y. P.; Yang, Y. C.; Klippenstein, S. J.; Dunbar, R. C. *J. Phys. Chem.* **1997**, *101*, 3338.

(9) (a) Hoshino, K.; Kurikawa, T.; Takeda, H.; Nakajima, A.; Kaya, K. *J. Phys. Chem.* **1995**, *99*, 3053. (b) Judai, K.; Hirano, M.; Kawamata, H.; Yabushita, S.; Nakajima, A.; Kaya, K. *Chem. Phys. Lett.* **1997**, *270*, 23.

(10) Pozniak, B. P.; Dunbar, R. C. *J. Am. Chem. Soc.* **1997**, *119*, 10439.

(11) (a) Roth, L. M.; Huang, Y.; Schwedler, J. T.; Cassady, C. J.; Ben-Amotz, D.; Kahr, B.; Freiser, B. S. *J. Am. Chem. Soc.* **1991**, *113*, 6298. (b) Huang, Y.; Freiser, B. S. *J. Am. Chem. Soc.* **1991**, *113*, 8186. (c) Huang, Y.; Freiser, B. S. *J. Am. Chem. Soc.* **1991**, *113*, 9418. (d) Jiao, Q.; Huang, Y.; Lee, S. A.; Gord, J. R.; Freiser, B. S. *J. Am. Chem. Soc.* **1992**, *114*, 2726.

(12) Basir, Y.; Anderson, S. L. *Chem. Phys. Lett.* **1995**, *243*, 45.

(13) Welling, M.; Thompson, R. I.; Walther, H. *Chem. Phys. Lett.* **1996**, *253*, 37.

(14) (a) Martin, T. P.; Malinowski, N.; Zimmermann, U.; Naher, U.; Schaber, H. J. *J. Chem. Phys.* **1993**, *99*, 4210. (b) Zimmermann, U.; Malinowski, N.; Naher, U.; Frank, S.; Martin, T. P. *Phys. Rev. Lett.* **1994**, *72*, 3542. (c) Tast, F.; Malinowski, N.; Frank, S.; Heinebrodt, M.; Billas, I. M. L.; Martin, T. P. *Phys. Rev. Lett.* **1996**, *77*, 3529. (d) Tast, F.; Malinowski, N.; Heinebrodt, M.; Billas, I. M. L.; Martin, T. P. *J. Chem. Phys.* **1997**, *106*, 9372.

(15) (a) Reddic, J. E.; Robinson, J. C.; Duncan, M. A. *Chem. Phys. Lett.* **1997**, *279*, 203.

(16) Nakajima, A.; Nagao, S.; Takeda, H.; Kurikawa, T.; Kaya, K., *J. Chem. Phys.* **1997**, *107*, 6491.

(17) Birks, J. B., *Photophysics of Aromatic Molecules*; John Wiley: London, 1970.

(18) Klessinger, M.; Michl, J., *Excited States and Photochemistry of Organic Molecules*; VCH Publishers: New York, 1995.

(19) Allamandola, L. J.; Tielens, A. G. G. M.; Barker, J. R. *Astrophys. J.* **1985**, *290*, L25.

(20) Bohme, D. K. *Chem. Rev.* **1992**, *92*, 1487.

(21) (a) Cook, D. J.; Schlemmer, S.; Balucani, N.; Wagner, D. W.; Steiner, B.; Saykally, R. J. *Nature* **1996**, *380*, 227. (b) Cook, D. J.; Schlemmer, S.; Balucani, N.; Wagner, D. W.; Harrison, J. A.; Steiner, B.; Saykally, R. J. *J. Phys. Chem.* **1998**, *102*, 1465.

(22) Hudgins, D. M.; Sandford, S. A. *J. Phys. Chem.* **1998**, *102*, 353.

(23) Langhoff, S. R.; Bauschlicher, C. W.; Hudgins, D. M.; Sandford, S. A.; Allamandola, L. J. *J. Phys. Chem.* **1998**, *102*, 1632.

(24) Ehrenfreund, P.; d'Hendecourt, L.; Verstraete, L.; Léger, A.; Schmidt, W.; Defourneau, D. *Astron. Astrophys.* **1992**, *259*, 257.

(25) Salama, F.; Joblin, C.; Allamandola, L. J. *J. Chem. Phys.* **1994**, *101*, 10252.

(26) Ekern, S. P.; Marshall, A. G.; Szczepanski, J.; Vala, M. *J. Phys. Chem.* **1998**, *102*, 3498.

(27) Rohlfing, E. A.; Cox, D. M.; Kaldor, A.; Johnson, K. H. *J. Chem. Phys.* **1984**, *81*, 3846.

(28) Loh, S. K.; Hales, D. A.; Lian, L.; Armentrout, P. B. *J. Chem. Phys.* **1989**, *90*, 5466.

(29) Referring to the bonding and ionization energetics in Table 1, a cycle shows that ejection of Fe_2^+ (plus neutral coronene) from $[\mathrm{Fe}_2{-}\mathrm{coronene}]^+$ is lower in energy than atomic ejection (plus charged coronene) by more than 2.0 eV. Similarly, ejection of Fe_3^+ from $[\mathrm{Fe}_3{-}\mathrm{coronene}]^+$ is more than 3.5 eV lower in energy than elimination of atoms.

(30) Buchanan, J. W.; Grieves, G. A.; Flynn, N.; Duncan, M. A. Unpublished results.

(31) Morrison, W. H.; Ho, E. Y.; Hendrickson, D. N. *Inorg. Chem.* **1975**, *14*, 500.

(32) Astruc, D. *Tetrahedron* **1983**, *39*, 4027.